AIP | Journal of Applied Physics

Protocol for classical molecular dynamics simulations of nano-junctions in solution

Konstantinos Gkionis, Ivan Rungger, Stefano Sanvito, and Udo Schwingenschlögl

Citation: Journal of Applied Physics **112**, 083714 (2012); doi: 10.1063/1.4759291
View online: http://dx.doi.org/10.1063/1.4759291
View Table of Contents: http://scitation.aip.org/content/aip/journal/jap/112/8?ver=pdfcov
Published by the AIP Publishing

[This article is copyrighted as indicated in the article. Reuse of AIP content is subject to the terms at: http://scitation.aip.org/termsconditions. Downloaded to] IP: 134.226.254.162 On: Tue, 28 Jan 2014 11:47:52

Protocol for classical molecular dynamics simulations of nano-junctions in solution

Konstantinos Gkionis,[1] Ivan Rungger,[2] Stefano Sanvito,[2] and Udo Schwingenschlögl[1,a)]
[1]*KAUST, PSE Division, Thuwal 23955-6900, Kingdom of Saudi Arabia*
[2]*School of Physics and CRANN, Trinity College, Dublin 2, Ireland*

(Received 25 July 2012; accepted 25 September 2012; published online 19 October 2012)

Modeling of nanoscale electronic devices in water requires the evaluation of the transport properties averaged over the possible configurations of the solvent. They can be obtained from classical molecular dynamics for water confined in the device. A series of classical molecular dynamics simulations is performed to establish a methodology for estimating the average number of water molecules N confined between two static and semi-infinite gold electrodes. Variations in key parameters of the simulations, as well as simulations with non-static infinite gold surfaces of constant area and with anisotropically fluctuating cell dimensions lead to less than 1% discrepancies in the calculated N. Our approach is then applied to a carbon nanotube placed between the gold electrodes. The atomic density profile along the axis separating the slabs shows the typical pattern of confined liquids, irrespective of the presence of the nanotube, while parallel to the slabs the nanotube perturbs the obtained profile. © *2012 American Institute of Physics*. [http://dx.doi.org/10.1063/1.4759291]

INTRODUCTION

Advances in technology have brought nanoscale devices at the forefront of scientific research over the past decades. Among the several directions of current nanoscale research, applications of biological importance attract intense interest. Cancer marker detectors,[1] DNA sequencing devices[2] and various nanotube- and nanowire-based biosensors[3–5] are only a few examples of such applications. Due to the biological nature of these applications, it is often required that the relevant nanodevices operate in wet conditions, as opposed to other nanoelectronic applications. In this situation, the electrical response of a device is modified, and sometimes dominated, by the dynamical evolution of the solvent. As such this needs to be accurately described, in particular in situations of strong confinement.

Advances in computational speed and efficiency have significantly increased the size of molecular systems that can be simulated. For instance, classical molecular dynamics (MD) simulations can be applied for systems composed of thousands of atoms, thus allowing for theoretical investigation of a variety of systems. Several biomolecular systems,[6–8] fluids and liquids confined at the nanoscale[9] and transport through nanopores[10] are only a few examples that require numbers of atoms of such magnitude.

Similarly, inclusion of explicit solvent molecules is tractable even at the more computationally demanding level of ab initio calculations, allowing for solvent effects to be investigated with greater accuracy.[11] However, it is well established that liquids confined at the nanoscale exhibit properties different from those of their bulk solutions, as a result of their highly ordered density profiles. Therefore, one question arises: What is the appropriate number of water or other solvent molecules that should be used in higher-level simulations involving electrodes, such as the ab initio quantum transport calculations in Ref. 11, especially when the distance between the latter is kept fixed by a molecule joining the two electrodes?

The present article deals with the above question for the case of water confined between two gold slabs of equal size, using classical MD simulations. Although classical MD studies in the "isosurface-isothermal-isobaric" ensemble (NAPT)[12,13] deal with systems of confined liquids and are computationally efficient, they are not practical to use for answering the above question. Therefore, we attempt to establish a methodology that can be used as a preliminary step for the ab initio modeling. We compare the NAPT approach with the grand canonical MD method of Gao, Luedtke, and Landman[14] and examine possible edge effects due to the semi-infinite nature of the electrodes.

METHODS

Systems of four different sizes have been used throughout the entire discussion, for which the Cartesian axes are assumed as shown in Figure 1. The specific slabs displayed in this figure consist of five layers of gold atoms in the xy-plane with size approximately 1.9×1.6 nm. The two slabs are separated by 4.0 nm, while the total number of the Au atoms is 480 and that of the H_2O molecules is 1100, part of which is confined between the two electrodes. This system will be referred to as "small." The input simulation box with periodic boundary conditions is $5.0 \times 1.7 \times 6.3$ nm in size. Systems referred to as "large" and "triple" have identical y- and z-dimensions, while the x-dimension of the slab is two and three times larger than that of the small system (i.e., $3.8 \times 1.6 \times 6.0$ nm and $5.7 \times 1.6 \times 6.0$ nm, respectively). Consequently, the x-dimension of the simulation box and the total number of H_2O molecules are adjusted to 6 nm and 2000, respectively, for the large system and to 12.0 nm and 5000 for the triple system. All three systems are set up as

a)Author to whom correspondence should be addressed. Electronic mail: udo.schwingenschlogl@kaust.edu.sa.

 © 2012 American Institute of Physics

[This article is copyrighted as indicated in the article. Reuse of AIP content is subject to the terms at: http://scitation.aip.org/termsconditions. Downloaded to] IP: 134.226.254.162 On: Tue, 28 Jan 2014 11:47:52

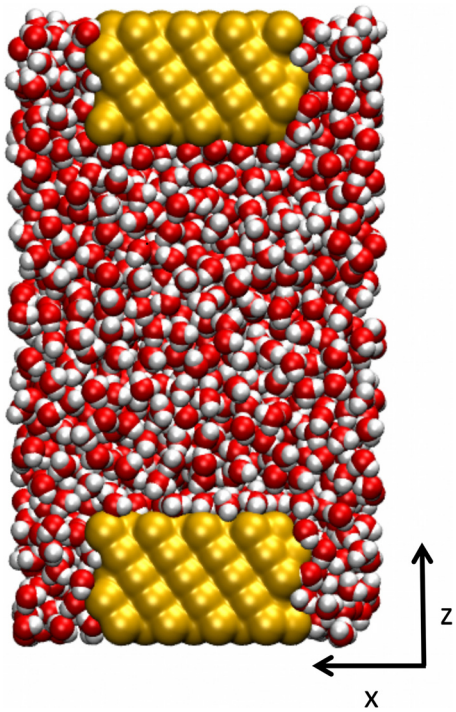

FIG. 1. Semi-infinite Au slabs (top and bottom) partially surrounded by water.

shown in Figure 1, i.e., the Au surfaces are semi-infinite with periodicity in the y-direction only. The thickness of 5 Au layers ensures that the confined water molecules do not interact with their periodic image along z, given the cutoff of the non-bonded interactions that is used in this study (see below).

The fourth system consists of a single 10-layer Au surface (1920 Au atoms) with approximate dimensions of $3.9 \times 3.3 \times 2.1$ nm and a $1.2 \times 1.2 \times 2.0$ nm rectangular water box of 250 molecules positioned some 0.4 nm above the Au surface. This system will be referred to as "surface-droplet" system. Its simulation box is $4.0 \times 3.4 \times 10.0$ nm. In this case, the z-dimension of the box is chosen to be 10 nm so as not to have interaction with the periodic image during the MD simulation. Details of the simulation box and Au slab sizes, as well as of the number of involved chemical species are summarized in Table I.

All simulations have been carried out with the NAMD2 software[15] and its CHARMM force-field[16] implementation. The resulting trajectories and images are analyzed and generated, respectively, using visual molecular dynamics.[17] In all cases, the TIP3P water model[18] is employed for the bonding and Lennard-Jones (LJ) parameters for the water molecules, with their intramolecular degrees of freedom kept constant. The gold atoms are neutral and kept fixed, unless otherwise stated, and qualitative comparisons are performed between the parameters of the universal force field (UFF)[19] force field and those of Heinz, Vaia, Farmer, and Naik,[20] hereafter called simply "HVFN" parameters. The carbon nanotube (CNT), when present, is neutral and its atoms are fixed in space and described by the parameters for aromatic carbon atoms of the CHARMM force field. Heteroatom LJ interaction potentials are based on the traditional Lorentz and Berthelot mixing rules for the minimum distance ($r_{min,ij}$) and epsilon (ε_{ij}) constants, respectively, i.e., an arithmetic mean for $r_{min,ij}$ and a geometric mean for ε_{ij}. Non-bonded van der Waals interactions among atoms separated by more than 1.0 nm are smoothly switched to vanish at 1.2 nm, beyond which distance they are incorporated as a correction.[21] Electrostatic interactions are computed using the Ewald summation[22] with the particle-mesh Ewald method.[23] The timestep of the simulations is 2 fs and the evaluation of the electrostatic interactions is performed every 4 fs.

Unless otherwise stated, all simulations are initiated by an energy minimization to eliminate possible steric clashes in the input structures. The following steps include heating of the system to 320 K at a rate of 0.5 K every 200 fs to overcome possible local barriers and then cooling to the desired temperature of 300 K at the same rate, in order to finally simulate the "isothermal-isobaric" ensemble (NPT).

Temperature control is achieved by the temperature reassignment method for the heating stage and by Langevin dynamics for the NPT stage. In all but one cases (accordingly mentioned in the Results section), a Langevin damping coefficient of $5\,ps^{-1}$ is applied for all atoms. In addition, pressure is controlled by the Nosé-Hoover method[24] and the piston fluctuation control implementation,[25] with a piston period of 400 fs and decay of 200 fs. Constant area (either xy or yz) is used in most of the simulations. In cases where the xy area is kept constant, the ensemble is $NA_{xy}\sigma_{zz}T$ (hereafter simply referred to as NAPT). In all other simulations, the yz area is kept constant and the Au slabs are in contact with water both on the xy and yz sides.

Finally, an NPT simulation is performed for 80 ns. It must be noted that at least in the case of water much shorter equilibration times should be adequate. We chose this simulation length in order to examine issues associated with the use of controlled pressure in combination with fixed atoms.[26,27] Equilibration of the systems is monitored using running averages and averaging the properties at different time blocks of the trajectories. The latter are recorded every 2 ps. The numbers N of water molecules reported in the following discussion are averaged over timeblocks of 5 ns, i.e., 2500 trajectory snapshots, while the number of water molecules of an individual snapshot is denoted as N_i.

TABLE I. Sizes and particle numbers of the model systems.

System	Number of H_2O molecules	Number of Au atoms	Simulation box (nm)	Au slab (nm)
Small	1100	480	$5.0 \times 1.7 \times 6.3$	$1.9 \times 1.6 \times 6.0$
Large	2000	960	$6.0 \times 1.7 \times 6.3$	$3.8 \times 1.6 \times 6.0$
Triple	5000	1440	$12.0 \times 1.7 \times 6.3$	$5.7 \times 1.6 \times 6.0$
Surface-droplet	250	1920	$4.0 \times 3.4 \times 10.0$	$3.9 \times 3.3 \times 2.1$

[This article is copyrighted as indicated in the article. Reuse of AIP content is subject to the terms at: http://scitation.aip.org/termsconditions. Downloaded to] IP: 134.226.254.162 On: Tue, 28 Jan 2014 11:47:52

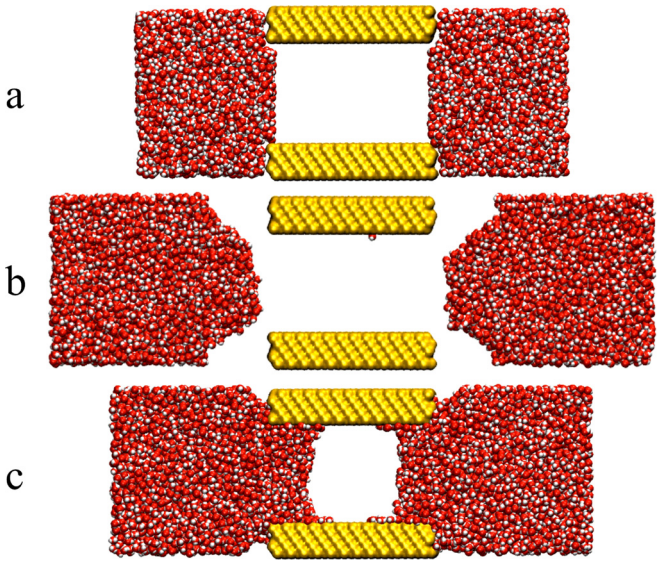

FIG. 2. (a) Input configuration. (b), (c) Result after heating using UFF and HVFN parameters, respectively.

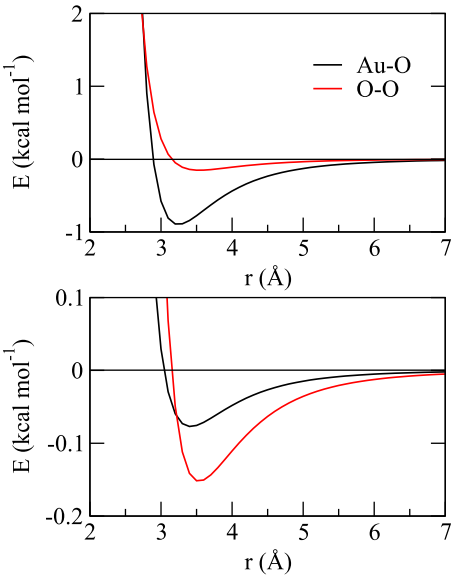

FIG. 4. Comparison of the O-O (TIP3P) Lennard-Jones interaction potential with the Au-O potential that results from combination rules between van der Waals parameters for O and HVFN (top) and UFF (bottom) parameters for Au.

RESULTS

Preliminary calculations have been carried out in order to test the two sets of Lennard-Jones parameters for Au (UFF and HVFN) on their ability to capture essential qualitative aspects of the Au-water system. The HVFN parameters have been optimized especially for face-centered cubic metals, while the UFF for positively charged Au atoms (Au^{3+}). Yet, UFF has been used for the description of uncharged Au atoms.[11,28–30] Taking the example of a NAMD2 case study,[31] the quality of the employed Lennard-Jones parameters for a surface can be tested by checking whether water will move through a nanopore of the given material. Setting up the small and the triple system (see Methods section) as shown in Figure 2(a), we observe for the UFF parameterization of the Au atoms that the water molecules move in the opposite direction of the nanopore, increasing their distance from the Au slabs, both for the small and the larger system (Figure 2(b)). In contrast, when switching to the HVFN parameters the water molecules completely fill the nanopore during the minimization process in the case of the small system. For the larger system, the filling of the nanopore by water is initialized again in the minimization step and continues during the subsequent heating step. At this stage, when the different phases coexist it can be observed that the water molecules near the Au surface move with greater velocity (Figure 2(c)), leading to an almost semi-ellipsoidal shape of the free space between the left and right water domains, an effect reminiscent of the "almost hemispherical" shape that has been reported for surface tension studies.[32] The filling process is completed after about 190 ps of the NPT simulation. This behavior is consistent with the hydrophilic nature of Au surfaces.[33]

The second qualitative test concerns the behavior of a water droplet on top of an Au surface, for which the surface-droplet system is employed (see Methods section). It is well established that the Au surface (free of impurities) is spontaneously wetted by water, an effect that is manifested by the measured contact angles between the water droplet and the surface.[34,35] Again, the qualitative differences between the

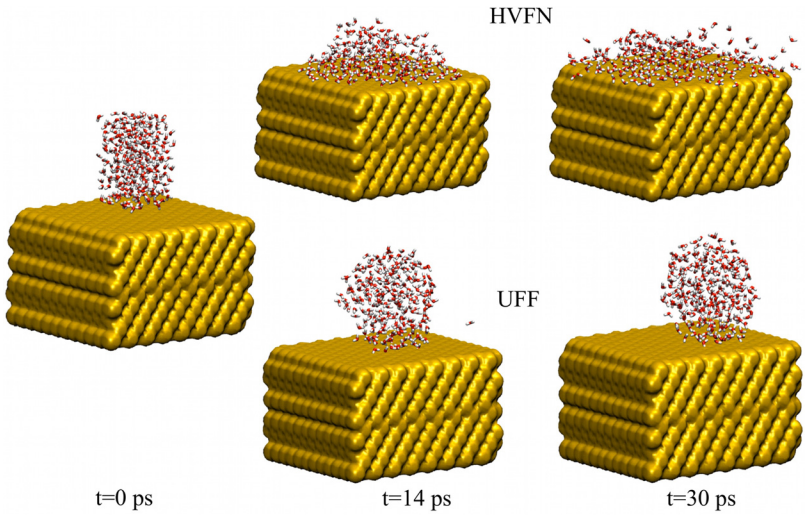

FIG. 3. Behavior of a water droplet on an Au(111) surface, calculated by using either the HVFN (top) and UFF (bottom) parameters.

[This article is copyrighted as indicated in the article. Reuse of AIP content is subject to the terms at: http://scitation.aip.org/termsconditions. Downloaded to] IP: 134.226.254.162 On: Tue, 28 Jan 2014 11:47:52

two sets of parameters are fundamental: Whereas the HVFN parameters result in wetting the Au surface, a non-wetting behavior is observed for the UFF parameters. Figure 3 displays two snapshots of the Au-water interface at 14 and 30 ps. At 14 ps, the droplet is already deformed with the water molecules expanding across the surface, which is covered by water at 30 ps. During the same time, a non-wetting behavior is observed for the UFF, where the droplet seems to slide across the surface.

Whether this motion is the slipping observed for droplets on hydrophobic surfaces[36] (recent results exhibit the possibility for this phenomenon to occur for hydrophilic surfaces as well[37]) is beyond the scope of the present work, as is a full quantitative analysis of the dynamics of the two examples above. However, the hydrophobic/hydrophilic behavior that is observed for the two different sets of parameters could be envisaged by the Au-O interatomic potentials (Figure 4). The latter result from the application of the Lorentz-Berthelot combination rules for the metallic and the TIP3P parameters for oxygen in our study, i.e., a geometric mean for ε_{ij} (Berthelot) and an arithmetic mean for σ_{ij} (Lorentz). Between the two parameter sets, a weaker Au-O interaction is predicted in the case of the UFF, a fact that is not surprising given the striking difference of the ε_{ii} values for the Au atoms. However, a qualitative feature that stems from this difference is that the Au-O potential is less attractive than the O-O potential when the UFF is considered, thus falsely ascribing hydrophobic properties to the Au surface. Consequently, due to the dominating O-O interaction, the clustering of water molecules among themselves, while repelled from the surface, appears energetically more favourable. The metal substrate is avoided in both of the above examples, as opposed to the more hydrophilic set of HVFN parameters.

The qualitative tests discussed so far led us to conclude that the UFF parameters are not suited to describe Au electrodes, so that we exclude this parameterization from subsequent comparisons. At this point, it should be noted that the above tests were performed only for gaining insights into the hydrophilic/hydrophobic behavior. The extensive discussion of the HVFN parameterization in Refs. 20 and 38 shows that these parameters are suitable. Additionally, the water parameterization can also have an effect on the results. However,

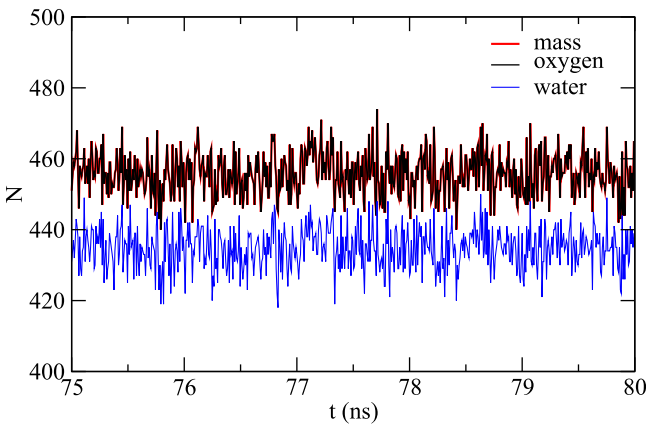

FIG. 5. Fluctuation of the number of water molecules in the selected volume of interest for the last 5 ns of the trajectory.

TABLE II. Number N and standard deviation of water molecules averaged over various time blocks and for different selection criteria.

Selection	Time-block (ns)	N	Standard deviation
Water	5–10	434	6
Water	40–45	435	6
Water	45–50	435	6
Water	70–75	435	6
Water	75–80	435	6
Oxygen	5–10	456	6
Oxygen	40–45	455	6
Oxygen	45–50	455	6
Oxygen	70–75	456	6
Oxygen	75–80	456	6
Mass	5–10	455	6
Mass	40–45	455	6
Mass	45–50	455	6
Mass	70–75	455	6
Mass	75–80	456	6

differences between standard water force-fields are significantly smaller than those observed between the UFF and HVFN parameterizations. Therefore, we excluded an analysis of different water models and only consider TIP3P water in order to compare with previous results (see Ref. 11).

We proceed with the suitable hydrophilic parameters. Initially, a simulation for the small system (see Methods section) was performed using a long-range correction to the van der Waals interactions and a Langevin constant of $5\,ps^{-1}$. This specific setup will be denoted as "S1". The first issue that one has to face when estimating the average number of molecules in the simulation volume is the water selection criterion. In other words, one has to establish a rule for deciding whether a given molecule is inside or outside the volume. In our case, we consider the volume that is enclosed by the Au electrodes. As shown in Figure 5, N_i fluctuates during the course of the trajectory, while the volume of interest is specific and constant. Selecting only the "whole" water molecules present in this volume would underestimate N_i and its average, since molecules that have only the oxygen or only one/two hydrogen atoms in the volume would be excluded from our estimates. Indeed, approximating N_i by counting only oxygen atoms that belong to the volume markedly shifts N_i to greater values (Figure 5 and Table II). A third selection criterion is the total mass that is enclosed in the volume at each snapshot (therefore counting all individual atoms). This mass is then used to estimate the N_i values. In this last case, the resulting graph (mass) is, not surprisingly, almost identical to the "oxygen" graph, since the oxygen atom is responsible for almost 90% of a water molecule's mass and the additional hydrogen atoms do not increase the N_i values dramatically.

The average N of N_i and the corresponding standard deviations for each of the above three selection criteria have been estimated for 5 ns at different time blocks of the 80 ns NPT trajectory and are shown in Table II. Both N and standard deviations are rounded to an integer value. It can be seen that for all the three selection criteria N remains practically constant for the different time blocks. Only slight

[This article is copyrighted as indicated in the article. Reuse of AIP content is subject to the terms at: http://scitation.aip.org/termsconditions. Downloaded to] IP: 134.226.254.162 On: Tue, 28 Jan 2014 11:47:52

fluctuations of 1 molecule are observed, which is negligible as compared to the standard deviation. The latter is found to maintain a constant value of 6 water molecules, irrespective of the time block and the selection considered. By comparing N for the different selection criteria, it is seen that the average of 435 water molecules for the "water" selection is raised to approximately 455 for the other two criteria. This increase of 4.6% corresponds to the mass excluded when the first selection criterion is applied, as discussed above. For our further discussion, we chose to employ the "mass" criterion and the time block of sampling to be 75-80 ns.

In the next step, we perform a series of additional simulations (S2-S6) using the small system (see Methods section) in order to examine how various factors affect the average number of water molecules N in the volume of interest throughout the MD trajectory. As we use the same pressure and temperature in all the calculations, N could be expected to depend on simulation parameters that can affect the density. Therefore, we test the effect of incorporating or omitting the correction to long-range van der Waals interactions (S1 and S2, respectively). This correction has an effect on the calculated densities.[21] N may also depend on the Langevin constant of the thermostat, since this acts as a friction to the system and affects the diffusion phenomena. Therefore, one additional simulation is performed in which the Langevin constant is reduced to $2\,ps^{-1}$ (S3). Finally, we estimate N in two additional ways: firstly by performing a canonical ensemble simulation in a box of constant volume and with its x-dimension enlarged to 6.5 nm (S4) and secondly by removing the temperature and pressure controls of the S1 system, i.e., by switching to a microcanonical ensemble for 2 ns (S5).

Table III summarizes the calculated N for each of the above cases. It is clear that changing the simulation parameters does not lead to significant deviations in the calculated N, which in most cases varies between 456 and 458. An exception is observed only when the long-range corrections to the truncated LJ potential are omitted (N = 449). This is an expected fact due to the effects of the correction on the calculated densities, as mentioned above. A similar result (N = 448) is obtained when the simulation box is expanded along the x-direction and no pressure control is applied. In summary, given that the standard deviation in N is 6 H_2O molecules in all cases, the observed differences are minor.

Table III includes results of two simulations using the large slabs (S6 and S7). In the former, all the parameters are identical to the S1 simulation and N is estimated for a volume in which the xy-area matches that of the small slab. In the latter, all the Au atoms apart from the two outer layers

TABLE III. Estimates of N and density for the different types of simulation and input parameters.

	S1	S2	S3	S4	S5	S6	S7
LJ correction	Yes	no	yes	yes	yes	yes	yes
Langevin constant (ps^{-1})	5	5	2	5	5	5	5
N	456	449	456	458	448	457	457
Standard deviation	6	6	6	6	5	6	6
Density (gr/cm^3)	0.993	0.978	0.992	0.976	0.997	0.996	0.995

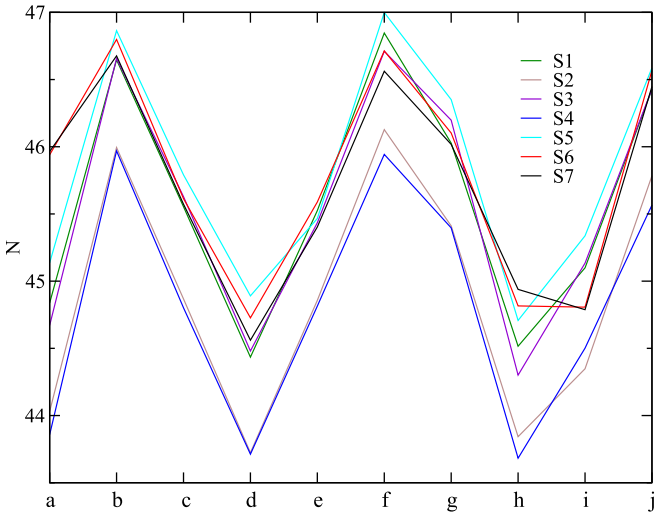

FIG. 6. Variation of the number N along the x-axis, based on bins of equal size (a-j).

are allowed to move. In both cases, the resulting N remains practically the same, indicating that the finite boundaries of the slab along x do not introduce any significant edge effects and the use of fixed Au atoms does not lead to a measurable reduction in the volume that is available to the free atoms. However, it must be noted that the main reason for using the large slab is the following: our target system consists of the small slab with periodic boundary conditions in all three dimensions, i.e., the xy area of the target unit cell is slightly larger than the actual slab area. The number N as estimated so far for the small slab does not account for this additional volume. The xy area in the above estimates of N is equal to the area of the Au layer that is in contact with the water. Using the large slab allows us to estimate N using the xy-area determined by the respective dimensions of the target unit cell. Hence, using the large slab and taking into account the above consideration results in a final value of N = 477.

In order to gain further insight into possible boundary effects due to the usage of a semi-infinite electrode, we examine how the N values of Table II are distributed along the x-axis. For this purpose, we divide the volume of interest in 10 equally spaced bins (a-j) along the x-axis. Although the

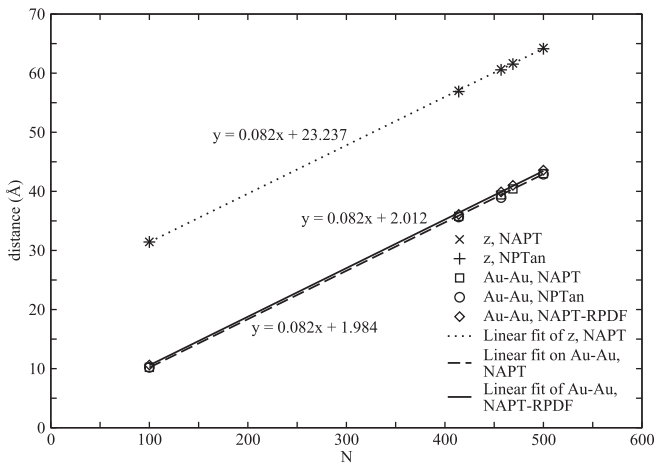

FIG. 7. Linear fits of the z and Au-Au distances against N.

[This article is copyrighted as indicated in the article. Reuse of AIP content is subject to the terms at: http://scitation.aip.org/termsconditions. Downloaded to] IP: 134.226.254.162 On: Tue, 28 Jan 2014 11:47:52

resulting deviations are small ($\pm 1\,H_2O$ molecule), they are maintained for all the simulations, as displayed in Figure 6, i.e., irrespective of the input parameters and the size of the slab. A minor discrepancy between the obtained trends is found for the simulations for the larger slab (see bins h to j). However, the differences are so small that further analysis was deemed unnecessary.

Having examined the possible sources of errors, we further employ the small system for calculations with constant xy area, as in the NAPT method for confined liquids, and calculations that allow anisotropic cell fluctuations (here after referred to as NAPTan for simplicity). In these calculations, the z-dimension of the cell varies with the number N of the H_2O molecules, where N = 100, 414, 457, 469, and 500. The remaining simulation parameters are the same as for LJ cor. and large. The z-dimension of the system is plotted against N in Figure 7 for both the NAPT and the NAPTan approaches. Furthermore, the Au-Au separation along z is plotted against N in the same figure. The Au-Au separation is estimated (i) by averaging the distance between the centers of mass of the inner layers of the two slabs ("Au-Au" in Figure 7) and (ii) from a radial pair distribution function (Au-Au(RPDF)) between two individual Au atoms.

In all three cases, we find a linear increase with N. The obtained linear fits have practically identical slopes and the intercepts with the distance axis are found to be reasonable for the limiting cases of N = 0. In addition, in both plots the points for NAPT and anisotropic are indistinguishable, indicating that the two approaches are equivalent. Finally, in comparison to our previous approach where N = 477 was determined, all linear fits of Figure 6 result in N = 482 for the same z- and Au-Au distance. This difference of 5 water molecules is within the standard deviation of our approach. The error is less than 1%. Thus, we conclude that the approach we follow for obtaining the number of water or other solvent molecules is suitable to avoid trial-and-error NAPT calculations and to be applied when the latter are not useful, for example when a nanotube is mounted between the electrodes. However, it should be noted that the NAPT approach requires less atoms to be taken into account (no bulk water) and thus is significantly faster.

At this point, it is worth commenting on the errors due to the anisotropic nature of the systems in all the approaches employed. When the semi-infinite electrodes are partially surrounded by water, a slight increase in the calculated N is observed if the simulation box is expanded along the x-direction (S4), thus eliminating interactions with periodic images along x. Although the difference is deemed insignificant compared to the observed standard deviation, it seems to be linked to interactions with periodic image along this axis. A second source of error is the summation of the electrostatic interactions (using the PME method) along the z direction. This fact has been correctly taken into account in Ref. 9 where the summation along z was omitted, and can explain why the intercepts of the linear fits in Figure 7 are not ideal. However, we have omitted a more sophisticated treatment, since all the simulations among which we compare contain the same error. Based on the above, the small differences between our approach and both the NAPT and anisotropic fluctuations approaches are likely to stem from changes in the electrostatic and van der Waals interactions due to both the different anisotropy and different number of water molecules. Yet, despite these sources of error, the observed differences are small enough to serve our purpose. Furthermore, for other solvents with larger molar volumes than water, the standard deviation is expected to decrease.

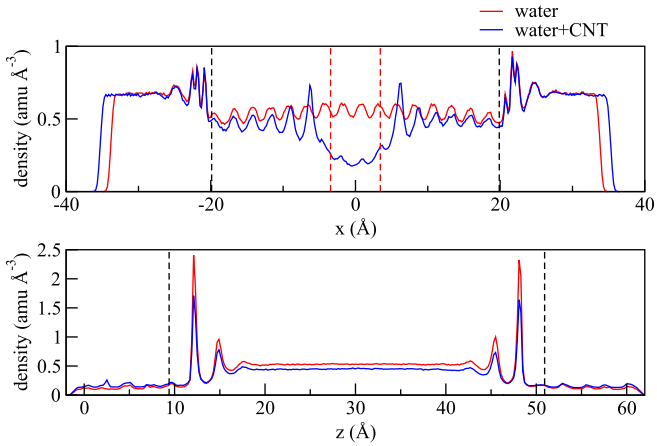

FIG. 8. Water density profiles along x (top) and along z (bottom) with and without the CNT.

Finally, we have applied the above procedure to a (8,0) carbon nanotube of length 3.7 nm sandwiched between the two Au slabs. The resulting number of water molecules is N = 369 with a standard deviation of 5. Since the interface of water with both the Au slabs and the nanotube in this case is of special interest, we comment on the orientation of the water molecules as well as on density profiles along the x- and z-axes, calculated with and without the nanotube. The density profiles are shown in Figure 8. The density along the z-axis shows the typical profile of confined water, i.e., an increased concentration near the Au. This profile is not affected by the presence of the nanotube. In contrast, the subtle oscillations that occur along the x-axis (also observed in Figure 6) are similar in the two cases. However, in the case of the nanotube they become more pronounced as one gets closer to the tube (which is marked with red dashed lines in Figure 8), in accordance with the distributions observed for uncharged carbon nanotubes.[39] The effect of the tube on the profile of water does not extend beyond 10 Å from the tube. The peaks in the profile nearly coincide for the two cases. Beyond the boundaries of the slabs (shown as black dashed lines), the profiles along x are identical. Finally, in the region beyond the slabs' boundaries where the profile is nearly flattened, the density of the water is found to be around 0.66 amu Å^{-3} (where amu = atomic mass units) with a tendency to drop away from the slab boundaries. This value corresponds to 1.095 g cm^{-3} and is close to the bulk value. It must also be noted that the density profile along x has been estimated for a rectangular box with z dimension equal to the gap between the slabs. Therefore, the small unoccupied volume that exists between the slabs and the water molecules (since the slabs are not touched by the water molecules) is the cause for the "drop" in the density of water that is confined between the slabs compared to the that of the water outside.

[This article is copyrighted as indicated in the article. Reuse of AIP content is subject to the terms at: http://scitation.aip.org/termsconditions. Downloaded to] IP: 134.226.254.162 On: Tue, 28 Jan 2014 11:47:52

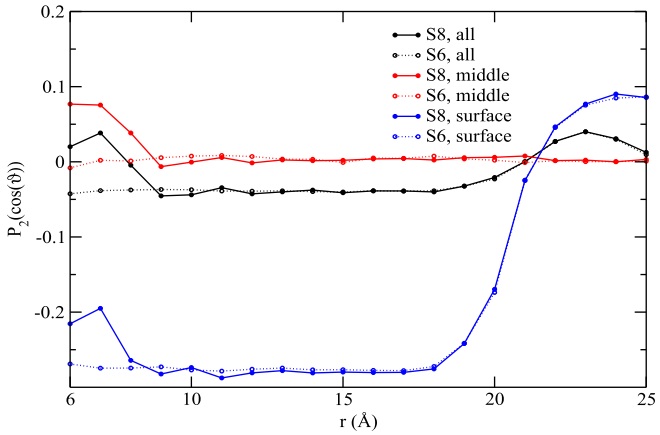

FIG. 9. Order parameter as a function of the distance from the center of the nanotube (r) for different spatial regions in the presence (S8) and absence (S6) of a nanotube.

Another feature related to the structural order of the systems is the orientation of the water molecules. This can be estimated in a similar manner as in Ref. 9 by the order parameter

$$P_2(\cos(\theta)) = \frac{3}{2}\langle \cos^2(\theta)\rangle - \frac{1}{2} \quad (1)$$

where θ is the angle between the z axis and a vector along the principal symmetry axis of the water molecules. The order parameter is calculated for the S6 and S8 systems. In order to gain insight into the effects of both the nanotube and the surface in system S8, $P_2(\cos(\theta))$ is calculated for cylindrical slices of 1 Å thickness around the nanotube in three different regions: the whole system ("all"), a slab of 5 Å thickness vertical to the nanotube in the middle between the electrodes ("middle"), and adjacent to the surfaces ("surface"). For comparison, the system S6 is analyzed in the same manner and the results are displayed in Figure 9. It can be seen that the ensemble average over the slice in the middle of the system yields $P_2(\cos(\theta)) = 0.0$, which implies a random orientation of the water molecules. A finite value occurs when the nanotube is present, and gradually drops to 0.0 for distances greater that 8-9 Å from the tubes central axis. The same difference between S6 and S8 (but less pronounced) is observed when considering the average of $P_2(\cos(\theta))$ for all the water molecules: The presence of the nanotube has effects up to the same distance from the axis, beyond which it matches the average of approximately -0.05 of the S6 system. This deviation from zero (and thus from a more strictly random orientation) when all water molecules are considered stems from the effect of the surface on the first layer of water, as observed from the respective profile of $P_2(\cos(\theta))$. The obtained average is consistently negative (between -0.25 and -0.3). Moreover, the perturbations due to the nanotube are similar to those described before. Note that the first data point of the S8-"surface" graph corresponds to water molecules that are exactly at the nanotube-Au junction. The first data point of the S8-"all" graph corresponds to the first layer of water around the nanotube. It is evident from the plot that there are rather small differences in the adopted orientations in the considered cases and regions. For longer distances (20 to 25 Å) from the principal axis of the nanotube noise is observed in all the plots due to the finite size of the Au electrodes along the x-axis and the fact that water molecules wet the sides of the electrodes. Thus, it is not surprising that for the "middle" slice $P_2(\cos(\theta))$ remains practically unaltered.

CONCLUSIONS

A series of classical molecular dynamics calculations has been employed in order to determine the average number of water molecules between two gold electrodes. A qualitative investigation of the available Lennard-Jones parameters for gold showed that the UFF parameters fail to describe key phenomena related to the surface, like the hydrophilic properties. In contrast, using the parameters of Heinz *et al.*[20] the studied systems show the expected behavior, i.e., first it allows water to enter between two gold slabs irrespective of the size of the latter, and second, it shows wetting when a water droplet is in contact with a gold surface. The different behavior observed for the different parameter sets can be explained on the basis of the shape of the Lennard-Jones potentials for heteroatom interactions, using combination rules.

The estimated number of water molecules N between two gold slabs separated by a given distance in practice does not vary whether or not the slabs are treated as static. Similarly, sampling under the NPT or NVE ensemble and changing the Langevin damping constant lead to little variation, much less than the associated statistical errors. The estimated N thus seems to be more affected by the corrections to the truncated van der Waals interactions and by the periodic boundary conditions. However, in all cases, the observed differences in N are less than 1%. Most importantly, and since no significant edge effects are present, in order to calculate the suitable number of water molecules to be used in the target unit cell, the slab's dimension along x must be at least equal to the respective lattice constant of the target system.

Similar differences are observed when the number N is obtained by linear regression against data points of given N and variable inter-surface distances. Furthermore, the results are virtually identical when derived via constant area calculations and less restrained calculations that allow for anisotropic fluctuations of the cell. This shows that the latter two trial-and-error approaches for estimating N, while not useful for the case of a sandwiched nanotube between electrodes, can also be avoided when only the solvent is present.

Finally, we have applied the followed approach to a carbon nanotube sandwiched between the two gold electrodes, a case in which the constant area and anisotropic fluctuations approaches would be difficult to apply. The number N is found to be much lower, since much of the volume is occupied by the nanotube. In contrast, the typical density profile of water confined between surfaces, perpendicular to the surfaces, is preserved in the presence of the nanotube.

ACKNOWLEDGMENTS

One of the authors (K.G.) would like to thank Dr. C. Cucinotta for useful discussions.

[This article is copyrighted as indicated in the article. Reuse of AIP content is subject to the terms at: http://scitation.aip.org/termsconditions. Downloaded to] IP: 134.226.254.162 On: Tue, 28 Jan 2014 11:47:52

[1]M. Ferrari, Nat. Rev. Cancer **5**, 161–171 (2005).
[2]P. K. Gupta, Trends Biotechnol. **26**, 602–611 (2008).
[3]F. Patolsky, G. Zheng, and C. M. Lieber, Anal. Chem. **78**, 4260–4269 (2006).
[4]B. He, T. J. Morrow, and C. D. Keating, Curr. Opin. Chem. Biol. **12**, 522–528 (2008).
[5]S. Roy and Z. Gao, Nano Today **4**, 318–334 (2009).
[6]T. E. Cheatham III and B. R. Brooks, Theor. Chim. Acta. **99**, 279–288 (1998).
[7]W. Wang, O. Donini, C. M. Reyes, and P. A. Kollman, Annu. Rev. Biophys. Biomol. Struct. **30**, 211–243 (2001).
[8]J. Norberg and L. Nilsson, Q. Rev. Biophys. **36**, 257–306 (2003).
[9]K. Johnston and V. Harmandaris, J. Phys. Chem. C **115**, 14707–14717 (2011).
[10]U. F. Keyser, J. R. Soc. Interface **8**, 1369–1378 (2011).
[11]I. Rungger, X. Chen, U. Schwingenschlögl, and S. Sanvito, Phys. Rev. B **81**, 235407 (2010).
[12]J. C. Wang and K. A. Fichthorn, J. Chem. Phys. **112**, 8252–8259 (2000).
[13]H. Eslami, F. Mozaffari, J. Moghadasi, and F. Muller-Plathe, J. Chem. Phys. **129**, 194702 (2008).
[14]J. Gao, W. D. Luedtke, and U. Landman, J. Chem. Phys. **106**, 4309–4318 (1997).
[15]J. C. Phillips, R. Braun, W. Wang, J. Gumbart, E. Tajkhorshid, E. Villa, C. Chipot, R. D. Skeel, L. Kale, and K. Schulten, J. Comput. Chem. **26**, 1781–1802 (2005).
[16]A. D. MacKerell Jr., D. Bashford, M. Bellott, R. L. Dunbrack Jr., J. Evanseck, M. J. Field, S. Fischer, J. Gao, H. Guo, S. Ha, D. Joseph, L. Kuchnir, K. Kuczera, F. T. K. Lau, C. Mattos, S. Michnick, T. Ngo, D. T. Nguyen, B. Prodhom, I. W. E. Reiher B. Roux, M. Schlenkrich, J. Smith, R. Stote, J. Straub, M. Watanabe, J. Wiorkiewicz-Kuczera, D. Yin, and M. Karplus, J. Phys. Chem. B **102**, 3586–3616 (1998).
[17]W. Humphrey, A. Dalke, and K. Schulten, J. Mol. Graphics **14**, 33–38 (1996).
[18]W. L. Jorgensen, J. Chandrasekhar, J. D. Madura, R. W. Impey, and M. L. Klein, J. Chem. Phys. **79**, 926–934 (1983).
[19]A. K. Rappé, C. J. Casewit, K. S. Colwell, W. A. Goddard III, and W. M. Skiff, J. Am. Chem. Soc. **114**, 10024–10035 (1992).
[20]H. Heinz, R. A. Vaia, B. L. Farmer, and R. R. Naik, J. Phys. Chem. C **112**, 17281–17290 (2008).
[21]M. R. Shirts, D. L. Mobley, J. D. Chidera, and V. S. Pande, J. Phys. Chem. B **111**, 13052–13063 (2007).
[22]P. Ewald, Ann. Phys. **369**, 253–287 (1921).
[23]T. A. Darden, D. M. York, and L. G. Pedersen, J. Chem. Phys. **98**, 10089–10092 (1993).
[24]G. J. Martyna, D. J. Tobias, and M. L. Klein, J. Chem. Phys. **101**, 4177–4189 (1994).
[25]S. E. Feller, Y. Zhang, R. W. Pastor, and B. R. Brooks, J. Chem. Phys. **103**, 4613–4621 (1995).
[26]J. A. Yancey, N. A. Vellore, G. Collier, S. J. Stuart, and R. A. Latour, Biointerphases **5**, 85–95 (2010).
[27]W. Smith and P. M. Rodger, "The pressure in systems with frozen atoms" Collaborative Computational Projects 5 (CCP5) **2002** (http://www.ccp5.ac.uk/infoweb/wsmith22/wsmith22.pdf, accessed: 17/12/2011).
[28]A. R. Bizzarri, G. Constantini, and S. Cannistraro, Biophys. Chem. **106**, 111–123 (2003).
[29]J. Qian, R. Hentschke, and W. Knoll, Langmuir **13**, 7092–7098 (1997).
[30]Q. Pu, Y. Leng, X. Zhao, and P. T. Cummings, Nanotechnology **18**, 424007 (2007).
[31]T. A. Isgro, M. Sotomayor, and E. Cruz-Chu, "Case Study: Water and Ice" (http://www.ks.uiuc.edu/Training/CaseStudies/pdfs/water-1.pdf, accessed: 17/12/2011).
[32]R. Ransing, P. Dyson, P. M. Williams, and P. R. Williams, *Fluid Properties at nano/meso scale. A numerical treatment*; Wiley, 2008.
[33]J. Drelich and E. Chibowski, Langmuir **26**, 18621–18623 (2010).
[34]M. K. Bernett and W. A. Zisman, J. Phys. Chem. **74**, 2309–2312 (1970).
[35]T. Smith, J. Colloid Interface Sci. **75**, 51–55 (1980).
[36]J. P. Rothstein, Annu. Rev. Fluid Mech. **42**, 89–109 (2010).
[37]T. A. Ho, D. V. Papavassiliou, L. L. Lee, and A. Striolo, Proc. Natl. Acad. Sci. U.S.A. **108**, 16170–16175 (2011).
[38]J. Feng, R. B. Pandey, R. J. Berry, B. L. Farmer, R. R. Naik, and H. Heinz, Soft Matter **7**, 2113–2120 (2011).
[39]B. Huang, Y. Xia, M. Zhao, F. Li, X. Liu, Y. Ji, and C. Song, J. Chem. Phys. **122**, 084708 (2005).

[This article is copyrighted as indicated in the article. Reuse of AIP content is subject to the terms at: http://scitation.aip.org/termsconditions. Downloaded to] IP: 134.226.254.162 On: Tue, 28 Jan 2014 11:47:52